Polarization control of high order harmonics in the EUV photon energy range

Boris Vodungbo, Anna Barszczak Sardinha, Julien Gautier, Guillaume Lambert, Constance Valentin, Magali Lozano, Grégory Iaquaniello, Franck Delmotte, Stéphane Sebban, Jan Lüning, et al.

Polarization control of high order harmonics in the EUV photon energy range

Boris Vodungbo,[1,*] Anna Barszczak Sardinha,[1,2] Julien Gautier,[1] Guillaume Lambert,[1] Constance Valentin,[1] Magali Lozano,[1] Grégory Iaquaniello,[1] Franck Delmotte,[3] Stéphane Sebban,[1] Jan Lüning,[4] and Philippe Zeitoun[1]

[1]*Laboratoire d'Optique Appliquée, ENSTA ParisTech – CNRS – cole polytechnique, Chemin de la Hunire, 91761 Palaiseau , FRANCE*
[2]*Grupo de Lasers e Plasmas – Instituto de Plasmas e Fuso Nuclear, Instituto Superior Tcnico, Av. Rovisco Pais, 1049-001 Lisbon, PORTUGAL*
[3]*Laboratoire Charles Fabry de lInstitut dOptique, CNRS et Universit Paris Sud, Campus Polytechnique, RD 128, F-91127 Palaiseau, FRANCE*
[4]*Laboratoire de Chimie Physique – Matire et Rayonnement, Universit Pierre et Marie Curie – CNRS, 11 rue Pierre et Marie Curie, 75005 Paris, FRANCE*
**boris.vodungbo@ensta-paristech.fr*

Abstract: We report the generation of circularly polarized high order harmonics in the extreme ultraviolet range (18–27 nm) from a linearly polarized infrared laser (40 fs, 0.25 TW) focused into a neon filled gas cell. To circularly polarize the initially linearly polarized harmonics we have implemented a four-reflector phase-shifter. Fully circularly polarized radiation has been obtained with an efficiency of a few percents, thus being significantly more efficient than currently demonstrated direct generation of elliptically polarized harmonics. This demonstration opens up new experimental capabilities based on high order harmonics, for example, in biology and materials science. The inherent femtosecond time resolution of high order harmonic generating table top laser sources renders these an ideal tool for the investigation of ultrafast magnetization dynamics now that the magnetic circular dichroism at the absorption *M*-edges of transition metals can be exploited.

OCIS codes: (120.5410) Polarimetry; (340.7480) X-rays, soft x-rays, extreme ultraviolet (EUV).

References and links

1. I. McKinnie and H. Kapteyn, "High-harmonic generation: Ultrafast lasers yield X-rays," Nat. Photonics **4**, 149–151 (2010).
2. G. Lambert, J. Gautier, C. Hauri, P. Zeitoun, C. Valentin, T. Marchenko, F. Tissandier, J. Goddet, M. Ribiere, G. Rey, M. Fajardo, and S. Sebban, "An optimized kHz two-colour high harmonic source for seeding free-electron lasers and plasma-based soft X-ray lasers," N. J. Phys. **11**, 083033 (2009).
3. F. Krausz and M. Ivanov, "Attosecond physics," Rev. Mod. Phys. **81**, 163–234 (2009).
4. A. Morlens, J. Gautier, G. Rey, P. Zeitoun, J. Caumes, M. Kos-Rosset, H. Merdji, S. Kazamias, K. Cassou, and M. Fajardo, "Submicrometer digital in-line holographic microscopy at 32 nm with high-order harmonics," Opt. Lett. **31**, 3095–3097 (2006).

#139458 - $15.00 USD Received 9 Dec 2010; revised 30 Jan 2011; accepted 30 Jan 2011; published 22 Feb 2011

5. E. Papalazarou, D. Boschetto, J. Gautier, T. Garl, C. Valentin, G. Rey, P. Zeitoun, A. Rousse, P. Balcou, and M. Marsi, "Probing coherently excited optical phonons by extreme ultraviolet radiation with femtosecond time resolution," Appl. Phys. Lett. **93**, 041114 (2008).
6. G. Lambert, T. Hara, D. Garzella, T. Tanikawa, M. Labat, B. Carre, H. Kitamura, T. Shintake, M. Bougeard, S. Inoue, Y. Tanaka, P. Salieres, H. Merdji, O. Chubar, O. Gobert, K. Tahara, and M.-E. Couprie, "Injection of harmonics generated in gas in a free-electron laser providing intense and coherent extreme-ultraviolet light," Nat. Phys. **4**, 296–300 (2008).
7. P. Zeitoun, G. Faivre, S. Sebban, T. Mocek, A. Hallou, M. Fajardo, D. Aubert, P. Balcou, F. Burgy, D. Douillet, S. Kazamias, G. de Lachze-Murel, T. Lefrou, S. le Pape, P. Mercre, H. Merdji, A. S. Morlens, J. P. Rousseau, and C. Valentin, "A high-intensity highly coherent soft X-ray femtosecond laser seeded by a high harmonic beam," Nature **431**, 426–429 (2004).
8. R. Berlasso, C. Dallera, F. Borgatti, C. Vozzi, G. Sansone, S. Stagira, M. Nisoli, G. Ghiringhelli, P. Villoresi, L. Poletto, M. Pascolini, S. Nannarone, S. De Silvestri, and L. Braicovich, "High-order laser harmonics and synchrotron study of transition metals $M_{2,3}$ edges," Phys. Rev. B **73**, 115101 (2006).
9. C. La-O-Vorakiat, M. Siemens, M. M. Murnane, H. C. Kapteyn, S. Mathias, M. Aeschlimann, P. Grychtol, R. Adam, C. M. Schneider, J. M. Shaw, H. Nembach, and T. J. Silva, "Ultrafast demagnetization dynamics at the *M* edges of magnetic elements observed using a tabletop high-harmonic soft x-ray source," Phys. Rev. Lett. **103**, 257402 (2009).
10. K. Tiedtke, A. Azima, N. Bargen, L. Bittner, S. Bonfigt, S. Düsterer, B. Faatz, U. Frühling, M. Gensch, C. Gerth, N. Guerassimova, U. Hahn, T. Hans, M. Hesse, K. Honkavaar, U. Jastrow, P. Juranic, S. Kapitzki, B. Keitel, T. Kracht, M. Kuhlmann, W. B. Li, M. Martins, T. Nez, E. Plnjes, H. Redlin, E. L. Saldin, E. A. Schneidmiller, J. R. Schneider, S. Schreiber, N. Stojanovic, F. Tavella, S. Toleikis, R. Treusch, H. Weigelt, M. Wellhfer, H. Wabnitz, M. V. Yurkov, and J. Feldhaus, "The soft X-ray free-electron laser FLASH at DESY: beamlines, diagnostics and end-stations," N. J. Phys. **11**, 023029 (2009).
11. J. Arthur, G. Materlik, R. Tatchyn, and H. Winick, "The LCLS: A fourth generation light source using the SLAC linac," Rev. Sci. Instrum. **66**, 1987–1989 (2009).
12. M. Lewenstein, P. Balcou, M. Y. Ivanov, A. L'Huillier, and P. B. Corkum, "Theory of high-harmonic generation by low-frequency laser fields," Phys. Rev. A **49**, 2117–2132 (1994).
13. F. A. Weihe and P. H. Bucksbaum, "Measurement of the polarization state of high harmonics generated in gases," J. Opt. Soc. Am. B **13**, 157–161 (1996).
14. P. Dietrich, N. H. Burnett, M. Ivanov, and P. B. Corkum, "High-harmonic generation and correlated two-electron multiphoton ionization with elliptically polarized light," Phys. Rev. A **50**, R3585–R3588 (1994).
15. X. Zhou, R. Lock, N. Wagner, W. Li, H. C. Kapteyn, and M. M. Murnane, "Elliptically polarized high-order harmonic emission from molecules in linearly polarized laser fields," Phys. Rev. Lett. **102**, 073902 (2009).
16. M. Schledermann and M. Skibowski, "Determination of the ellipticity of light and of optical constants by use of two reflection polarizers," Appl. Opt. **10**, 321–326 (1971).
17. W. Westerveld, K. Becker, P. Zetner, J. Corr, and J. McConkey, "Production and measurement of circular polarization in the VUV," Appl. Opt. **24**, 2256–2262 (1985).
18. H. Höchst, R. Patel, and F. Middleton, "Multiple-reflection phase shifter: A viable alternative to generate circular-polarized synchrotron radiation," Nucl. Instrum. Methods Phys. Res. A **347**, 107–114 (1994).
19. D. Windt, "IMD – Software for modeling the optical properties of multilayer films," Comput. Phys. **12**, 360–370 (1998).

1. Introduction

High order harmonic generation (HHG) has attracted significant attention as a compact, femtosecond pulsed, coherent light source covering the extreme ultraviolet (EUV) photon energy range [1]. Femtosecond short pulses of a few nanojoules at a wavelength of 20 nm are now routinely achieved [2] and current efforts in source development are pushing towards even shorter wavelength and higher pulse energy. Using a fraction of the initial IR laser pulse as a pump, HHG sources are unique sources for IR pump - EUV probe experiments and thus ideal for the investigation of femtosecond dynamics. With such characteristics, it is not surprising that HHG sources have been used for numerous applications ranging from atomic and molecular physics [3], microscopy [4], phonon dynamics [5] and EUV metrology to "seeding" of EUV free electron lasers (FEL) [6] or EUV laser plasma amplifiers [7].

With the advent of HHG sources generating intense pulses in the spectral range above 50 eV (< 25 nm) it has become possible to perform with table top sources advanced core level spectroscopy techniques, a domain so far solely covered by large scale synchrotron radiation fa-

#139458 - $15.00 USD Received 9 Dec 2010; revised 30 Jan 2011; accepted 30 Jan 2011; published 22 Feb 2011

cilities. For example, Berlasso *et al.* [8] reported absorption spectroscopy experiments at the *M*-edges of 3d transition metals, which are located in this spectral range. The ability to reach these absorption resonances and the suitability of HHG sources for pump/probe experiments render them a powerful tool for the investigation of ultrafast magnetization dynamics occurring in 3d transition metals like Fe, Co and Ni. A first such experiment has been reported by La-O-Vorakiat *et al.* [9]. These authors exploited resonance effects of the spectroscopic absorption edges to follow ultrafast demagnetization dynamics in permalloy with element selectivity.

A second key advantage of EUV radiation with respect to IR or visible laser light is the significantly shorter wavelength, thus pushing the diffraction limit in photon based microscopy towards a few ten nanometers. Combining both aspects will enable time-resolved EUV spectro-microscopy experiments in the laboratory, thus overcoming the restrictions associated with large scale facilities. For example, it will be possible to study ultrafast magnetization dynamics with nanoscale resolution in many more places than the operating EUV and X-ray FEL [10,11].

Eventually, all magnetic microscopy techniques require circularly polarized light, since the magnetic contrast is given by the magnetic circular dichroism (MCD) of the absorption edges of transition metals. However, HHG sources deliver linearly polarized light when a linearly polarized driving laser is focused into an atomic gas. In that case, the high harmonic beam polarization follows the atomic dipole direction, which is directly related to the driving laser polarization [12].

Several attempts have been made to obtain circularly polarized harmonics. For example, already in the 1990's, it has been shown that using an elliptically polarized driving laser, elliptically polarized harmonics could be obtained [13]. The generation efficiency, however, drops dramatically with increasing ellipticity of the driving laser [14]. More recently, elliptically polarized harmonics have been obtained in molecular gases [15], but the degree of circular polarization is low (< 40 %). Moreover, efficient generation in molecular gases requires that the molecules are aligned. This adds complexity to the setup since a first laser pulse is needed to accomplish this task. We finally note that all previous studies have focused on rather low order harmonics and only sparse data are available for wavelengths lower than 25 nm.

In contrast to these previous reports, we chose a two-step procedure to obtain circularly polarized harmonics. First, linearly polarized harmonics are generated as efficiently as possible. A conversion efficiency of 10^{-7} has previously been measured for one harmonic at 18 nm with the same laser [2] but conversion efficiencies of up to 10^{-4} can be obtained [1]. Second, they are circularly polarized. In the visible and near UV region of the electro-magnetic spectrum circularly polarizing a linearly polarized light beam is easily done using quarter-wave plates. For wavelengths below 100 nm the situation is radically different since the lack of transparent materials prevents the fabrication of quarter-wave plates. However, the principle of an EUV circular polarizer has been discussed extensively and different designs have been proposed and realized [16–18].

The basic idea is to use the phase-shift introduced between the *s* and *p* component of an electromagnetic wave by a reflection on a mirror. To produce circularly polarized light from linearly polarized light, first of all, a phase-shift of $\frac{\pi}{2}$ must be introduced. Since the phase-shift introduced by a mirror ranges from 0, at grazing incidence, to π, at normal incidence, one can always find an incidence angle for which the phase shift is $\frac{\pi}{2}$ [17]. To obtain circularly polarized light, it is also necessary to adjust the direction of polarization of the incoming light so that after reflection the *s* and *p* components have equal intensity. Since the reflectivity of the *p* component is always lower than the one of the *s* component the angle between the electric field and the *p* direction (α_C angle) must be chosen between 0 and 45. Positive and negative helicity can be obtained using α_C and $-\alpha_C$.

In the EUV region, the incidence angle which gives a phase-shift of $\frac{\pi}{2}$ is in general close to

#139458 - $15.00 USD Received 9 Dec 2010; revised 30 Jan 2011; accepted 30 Jan 2011; published 22 Feb 2011

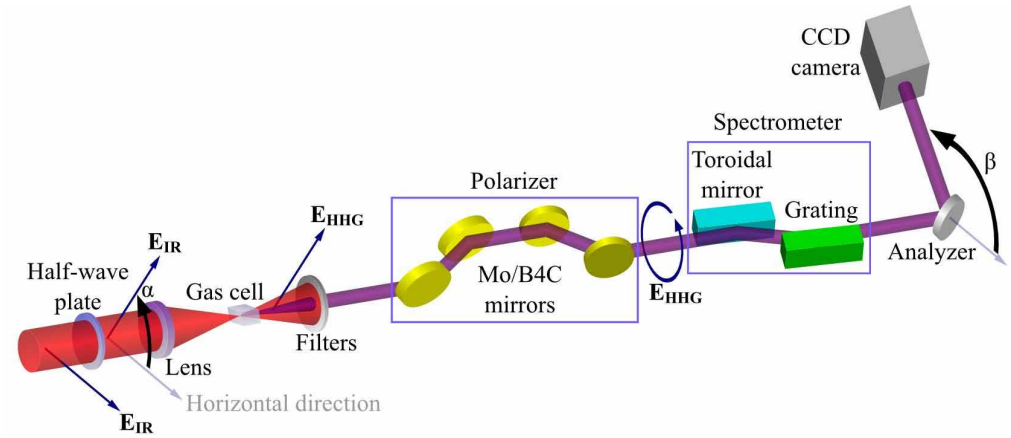

Fig. 1. Setup layout showing the production of the harmonics in a neon filled gas cell, the polarizer, the spectrometer, the analyzer and the CCD camera. At first, the infrared laser (red) is horizontally polarized. The polarization direction of the infrared laser is rotated by an angle α compared to the horizontal direction by an half-wave plate. The harmonics (purple) have the same polarization as the infrared laser. After the polarizer, the harmonics are elliptically polarized. They are focused and dispersed by the spectrometer. The harmonics are reflected by the analyzer and recorded on the CCD camera. The analyzer and the CCD camera can be rotated around the optical axis. The angle between the analyzer and the horizontal direction is noted β.

the Brewster angle. The reflectivity of the *p* component is then very low and this significantly lowers the efficiency of the polarizer. To overcome this difficulty, multiple mirror designs have been proposed. Since the phase-shift accumulates with each mirror, a smaller shift per mirror, hence, a smaller glancing angle can be used. This greatly improves the efficiency of the polarizer [18].

In this article we analyze the performance of a four mirror system used to circularly polarize the EUV pulses produced by an HHG source. In order to study the MCD effect at the cobalt *M*-edge, this system has been optimized for a wavelength of 20.7 nm (60 eV). The performance of the polarizer has been measured using a rotating analyzer consisting of a multilayer mirror set at an incidence angle of 45. In the following parts, we will describe the experimental setup, derive a theoretical model of the optical system and present our results.

2. Description of the experimental setup

Figure 1 is a sketch of our setup. High harmonics are generated by focusing 5 mJ, 40 fs (FWHM) pulses, from a Ti:Sapphire laser ($\lambda_0 = 815$ nm) operating at 1 kHz, into a gas cell filled with neon (25 mbar). These harmonics span a wide wavelength range between 16 and 31 nm and are linearly polarized in the same direction as the incoming infrared laser (i. e. horizontal, *p*-polarized). By rotating the direction of polarization of the infrared laser with a half-wave plate by an angle α, the direction of polarization of the harmonics can be rotated correspondingly (Fig. 1).

The polarizer consists of four mirrors, each coated with 35 nm of molybdenum capped with 5 nm of B_4C to prevent oxidation. Molybdenum has been chosen due to its high reflectivity and high phase-shift in the EUV range. The principle of a four mirror circular polarizer has been described elsewhere [18]. However, this system is simpler than the one of Hchst *et al.* The mirrors are fixed, which we can afford since we are interested in a particular photon energy and

#139458 - $15.00 USD Received 9 Dec 2010; revised 30 Jan 2011; accepted 30 Jan 2011; published 22 Feb 2011

since the plane of polarization of the incoming light can be rotated.

The polarizer was optimized to circularly polarized EUV radiation of 20.7 nm, matching the absorption *M*-edge of Co, using calculations performed with the optical constants of the IMD software package [19]. At this wavelength, the four reflector polarizer should yield a phase-shift of $\frac{\pi}{2}$ for a glancing angle of about 23.4. To obtain circularly polarized light an α angle of 32 is needed (α angle, Fig. 1), positive and negative helicity can be obtained using 32 or -32. The theoretical transmission should be 8 %, which is significantly higher than what a gold coated four reflector phase-shifter would yield (0.6 %) [18].

After the polarizer, the infrared light is filtered out by two 150 nm thick aluminum foils, which are highly transparent in the EUV spectral range. The harmonics are focused and dispersed by a platinum coated toroidal mirror working in conjunction with a 120 grooves per millimeter reflection grating. The harmonics are then reflected by a Mo/Si multilayer mirror set at an incidence angle of 45 and their intensity is recorded with a PI-MTE CCD camera (Princeton Instrument). The multilayer mirror has a period of 16 nm, a ratio of Mo and Si thicknesses of 0.6 and 20 repetitions. This mirror acts as an analyzer, the *s* and *p* reflectivities ratio changes from 6 to 16 for the brightest harmonics between 18 and 27 nm (31^{st} to 45^{th} harmonics). The multilayer mirror and the CCD camera can be rotated around the optical axis (angle β, Fig. 1).

Due to the dispersion introduced by the grating, the CCD camera records separately the intensity of each harmonic. A typical measurements consists of an accumulation of 40,000 pulses (i. e. 40 s). The intensities obtained for different α and β angles are dependent on the characteristics (reflectivity and phase-shift) of the different optical elements present in the setup. It is possible to retrieve these characteristics and to obtain the performance of the polarizer by fitting the intensities recorded on the CCD camera with a model describing the optical system. Theoretical considerations necessary to build this model are discussed in the following section.

3. Theoretical description of the optical system in the Stokes formalism

3.1. Reminders on Stokes parameters and Müller matrix

Consider a beam of light traveling along the *z* direction and the coordinate system given by three unitary vectors $\mathbf{z}$, $\mathbf{e_p}$ and $\mathbf{e_s}$ such as $\mathbf{z} = \mathbf{e_p} \times \mathbf{e_s}$. The electric field of the light $\mathbf{E}$ can be described by two complex numbers E_p and E_s:

$$\mathbf{E}(z,t) = (E_p \mathbf{e_p} + E_s \mathbf{e_s}) \exp(-\imath(\omega t - kz)). \tag{1}$$

The polarization state of the beam can be described by the Stokes vector, *S* which is defined as follows:

$$\begin{pmatrix} S_0 \\ S_1 \\ S_2 \\ S_3 \end{pmatrix} = \begin{pmatrix} \left(|E_p|^2 + |E_s|^2\right)/2 \\ \left(|E_p|^2 - |E_s|^2\right)/2 \\ \Re\left(E_p E_s^*\right) \\ \Im\left(E_p E_s^*\right) \end{pmatrix}. \tag{2}$$

S_0 is proportional to the intensity of the beam while the degree of linear polarization, P_L, and the degree of circular polarization, P_C, are related to the Stokes vector by the following equations:

$$P_L = \frac{(S_1)^2 + (S_2)^2}{(S_0)^2}, \tag{3}$$

$$P_C = \left(\frac{S_3}{S_0}\right)^2. \tag{4}$$

#139458 - $15.00 USD Received 9 Dec 2010; revised 30 Jan 2011; accepted 30 Jan 2011; published 22 Feb 2011

A rotation, of an angle ϕ, of the coordinate system around the z-axis is described by the rotation matrix $R(\phi)$:

$$\mathrm{R}(\phi) = \begin{bmatrix} 1 & 0 & 0 & 0 \\ 0 & \cos(2\phi) & \sin(2\phi) & 0 \\ 0 & -\sin(2\phi) & \cos(2\phi) & 0 \\ 0 & 0 & 0 & 1 \end{bmatrix}, \tag{5}$$

the rotated Stokes vector being $R(\phi)S$.

The interaction of the light with an optical element can be described by the Müller matrix M_x of this optical element. After the interaction, the Stokes vector becomes M_xS. In the case of a reflective element with complex reflective coefficients $\tilde{r}_{px} = r_{px}\exp(\imath\delta_{px})$ and $\tilde{r}_{sx} = r_{sx}\exp(\imath\delta_{sx})$ we have:

$$M_x = \frac{1}{2}\left(r_{px}^2 + r_{sx}^2\right)\begin{bmatrix} 1 & -\cos(2\Psi_x) & 0 & 0 \\ -\cos(2\Psi_x) & 1 & 0 & 0 \\ 0 & 0 & \sin(2\Psi_x)\cos(\Delta_x) & \sin(2\Psi_x)\sin(\Delta_x) \\ 0 & 0 & -\sin(2\Psi_x)\sin(\Delta_x) & \sin(2\Psi_x)\cos(\Delta_x) \end{bmatrix}, \tag{6}$$

where $\tan(\Psi_x) = \frac{r_{px}}{r_{sx}}$ and $\Delta_x = \delta_{px} - \delta_{sx}$. Δ_x represents the phase-shift induced by the optical element. A rotation, of an angle ϕ, of the optical element implies a coordinate transformation given by the rotation matrix $R(\phi)$, the resulting Mller matrix being $R(-\phi)M_xR(\phi)$.

3.2. Description of of the optical system

Consider one harmonic in a coordinate system such that the vector $\mathbf{e_p}$ and $\mathbf{e_s}$ are respectively chosen to be parallel and perpendicular to the plane of incidence of the circular polarizer (i. e. the horizontal plane). The harmonic being linearly polarized with its polarization plane rotated by an angle α compared to $\mathbf{e_p}$ (Fig. 1), the electric field of this harmonic is written:

$$\mathbf{E}(z,t) = (E_0\cos(\alpha)\mathbf{e_p} + E_0\sin(\alpha)\mathbf{e_s})\exp(-\imath(\omega t - kz)), \tag{7}$$

the corresponding Stokes vector being:

$$S_i = I_0\begin{pmatrix} 1 \\ \cos(2\alpha) \\ \sin(2\alpha) \\ 0 \end{pmatrix}, \tag{8}$$

where $I_0 = \frac{|E_0|^2}{2}$ is proportional to the intensity of the harmonic.

Let us divide the optical elements of our setup in two blocks. The first block is composed of the circular polarizer and the spectrometer (the toroidal mirror and the grating). This block is describe by a Mller matrix M_a, its parts being fixed compared to the coordinate system, no coordinate transformation is needed. Passing through this block, the Stokes vector is transformed into:

$$S_a = M_aS_i, \tag{9}$$

from which the degree of circular polarization can be retrieved:

$$P_C = \left(\frac{S_{a3}}{S_{a0}}\right)^2 = \frac{\sin^2(2\Psi_a)\sin^2(2\alpha)\sin^2(\Delta_a)}{\left(\cos(2\Psi_a)\cos(2\alpha) - 1\right)^2}. \tag{10}$$

Equation (10) shows that obtaining circular polarization, $P_C = 1$, requires a phase-shift, Δ_a, of $\frac{\pi}{2}$. Furthermore, the value of the angle α which maximizes P_C is Ψ_a. When the latter condition

#139458 - $15.00 USD Received 9 Dec 2010; revised 30 Jan 2011; accepted 30 Jan 2011; published 22 Feb 2011

is met the degree of circular polarization and the circular transmission are respectively:

$$P_C^{Max} = \sin^2(\Delta_a) \tag{11}$$

$$T_C = \frac{S_{a0} P_C^{Max}}{I_0} = \frac{(r_{pa}^2 + r_{sa}^2)\sin^2(2\Psi_a)\sin^2(\Delta_a)}{2}. \tag{12}$$

The circular transmission, T_C, can be seen as the ratio between the number of photons circularly polarized after the first block and the number of incident photons.

The second block is composed of the rotating analyzer and the CCD camera. This analyzer is described by a Mller matrix M_b. To take into account the orientation of the polarizer ,angle β, we need to proceed to a coordinate transformation. After this block, the Stokes vector becomes:

$$S_b = R(-\beta)M_b R(\beta)M_a S_i. \tag{13}$$

The CCD camera is sensitive to the intensity of the harmonics, i. e. the first component of the Stokes vector. In our case the CCD camera records:

$$S_{b0} = \frac{1}{4} I_0 (r_{pa}^2 + r_{sa}^2)(r_{pb}^2 + r_{sb}^2) \begin{pmatrix} +1 \\ -\cos(2\alpha)\left(\cos(2\Psi_a) + \cos(2\beta)\cos(2\Psi_b)\right) \\ -\sin(2\alpha)\sin(2\beta)\sin(2\Psi_a)\cos(2\Psi_b)\cos(\Delta_a) \\ +\cos(2\beta)\cos(2\Psi_a)\cos(2\Psi_b) \end{pmatrix}. \tag{14}$$

By varying α and β independently, and by fitting the measured data to expression (14), the values of Ψ_a, Δ_a, Ψ_b and $I_f = \frac{1}{4} I_0 (r_{pa}^2 + r_{sa}^2)(r_{pb}^2 + r_{sb}^2)$ can be retrieved.

It must be noted that the parameters Ψ_a and Δ_a describe a composite optical element which include the polarizer and the spectrometer. To calculate the performance of the polarizer only, we have to separate the contribution of the spectrometer, which reflection coefficient are $\tilde{r}'_{(p,s)a} = r'_{(p,s)a}\exp(\imath\delta'_{(p,s)a})$, from the contribution of the polarizer, which reflection coefficient are $\tilde{r}''_{(p,s)a} = r''_{(p,s)a}\exp(\imath\delta''_{(p,s)a})$. This is done by removing the polarizer and recording a new set of data. From this new measurements,$\Psi'_a = \arctan\left(\frac{r'_{pa}}{r'_{sa}}\right)$, $\Delta'_a = \delta'_{pa} - \delta'_{sa}$ and $I'_f = \frac{1}{4} I_0 (r'^2_{pa} + r'^2_{sa})(r_{pb}^2 + r_{sb}^2)$ can be retrieved. Remarking that $\tilde{r}_{s,pa} = \tilde{r}'_{s,pa}\tilde{r}''_{s,pa}$ and $\frac{I_f}{I'_f} = \frac{r_{pa}^2 + r_{sa}^2}{r'^2_{pa} + r'^2_{sa}}$ one can deduce:

$$\Delta''_a = \Delta_a - \Delta'_a, \tag{15}$$

$$r''_{sa} = \sqrt{\frac{I_f}{I'_f}\left(\frac{1+\tan^2(\Psi'_a)}{1+\tan^2(\Psi_a)}\right)}, \tag{16}$$

$$r''_{pa} = r''_{sa}\frac{\tan(\Psi_a)}{\tan(\Psi'_a)}. \tag{17}$$

P_C^{Max} and T_C can finally be calculated using r''_{pa}, r''_{sa}, $\Psi''_a = \arctan\left(\frac{r''_{pa}}{r''_{sa}}\right)$ and Δ''_a.

4. Experimental results

The intensity of each harmonic was recorded on the CCD camera for polarization angles, α, ranging from -200 to 220, and at four different analyzer angles, β, 0, 45, 90 and 135. Two sets of data were recorded, one with and the other without the 4 mirror polarizer. Figure 2(a) shows an image of the harmonics obtained with polarizer for $\alpha = 90$ and $\beta = 0$. A line profile through the eight harmonics is reproduced in Fig. 2(b). These can be identified as harmonics 31st to 45th

#139458 - $15.00 USD Received 9 Dec 2010; revised 30 Jan 2011; accepted 30 Jan 2011; published 22 Feb 2011

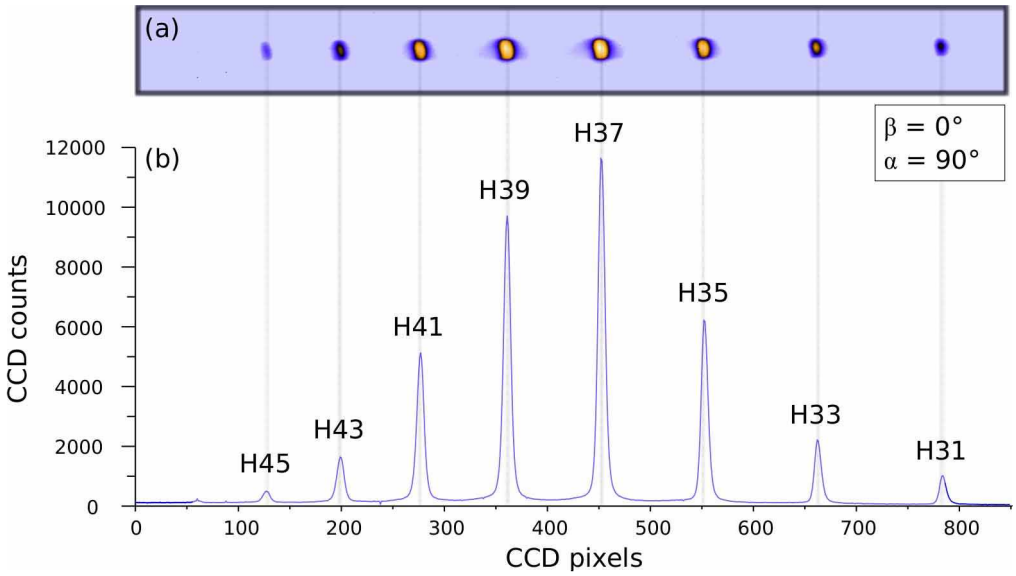

Fig. 2. (a) Image of the harmonic spectrum recorded on the CCD camera with the polarizer, for $\alpha = 90$ and $\beta = 0$. This image is an accumulation over 40,000 thousands pulses. For this α and β angles configuration, the harmonics intensities are maximum. (b) Cross section of the same image showing the intensity of each harmonic and the space (in pixels) between them. Using the grating characteristics (120 grooves/mm), the distance between the grating and the CCD camera and the space between the harmonics, each harmonic has been numbered. Eight harmonics are clearly visible, from the 31st to the 45th.

Table 1. Table summarizing the characteristics of the polarizer for each harmonic[1]

Harmonic order	31st	33rd	35th	37th	39th	41st	43rd	45th
λ (nm)	26.3	24.7	23.3	22	20.9	19.9	19	18.1
r''^2_{pa} (%)	1.5	1.6	2.5	2.7	3.8	4.3	4.5	4.5
r''^2_{sa} (%)	7.8	7.4	7.6	7.8	8.3	8.5	9.3	9.6
Δ''_a ()	87.6	85.2	80.5	72.3	67.2	60.4	54.4	51.1
P_{Cmax} (%)	100	100	97	91	85	76	66	61
T_C (%)	2.6	2.7	3.7	3.6	4.4	4.3	4.0	3.7

[1]The first line of the table shows the harmonic order while the second line shows the corresponding wavelength. For each harmonic, the reflectivies r''^2_{pa} and r''^2_{pa} the phase-shift Δ''_a the degree of circular polarization P_{Cmax} and the circular transmission T_C are displayed. The 39th harmonic at the Co absorption *M*-edge shows a degree of circular polarization of 85 % and a circular transmission of 4.4 %. For the 31st and 33rd harmonics, 100 % circularly polarized light is obtained with a transmission of 2.6 and 2.7 % respectively. For order superior to 39th, the degree of circular polarization remains higher than 61 % with a circular transmission higher than 3.7 %.

based on their respective spacing on the CCD camera, which is in line with the observation of the cut-off of the Al filters due to the Al K absorption edge at 17.1 nm.

The area below a peak gives the intensity of the corresponding harmonic. The intensity of each harmonic is then plotted as a function of α for the four β angles. The results obtained for the 39th harmonic (20.9 nm) are reproduced in Fig. 3. Without polarizer (Fig. 3(a)), the angular dependence is given by four sinusoids of approximately the same amplitude with a 45 phase shift between them. This behavior is expected if the phase-shift induced by the spectrometer is zero and the ratio of its *p* and *s* reflectivity is close to 1. We therefore can conclude that the

#139458 - $15.00 USD Received 9 Dec 2010; revised 30 Jan 2011; accepted 30 Jan 2011; published 22 Feb 2011

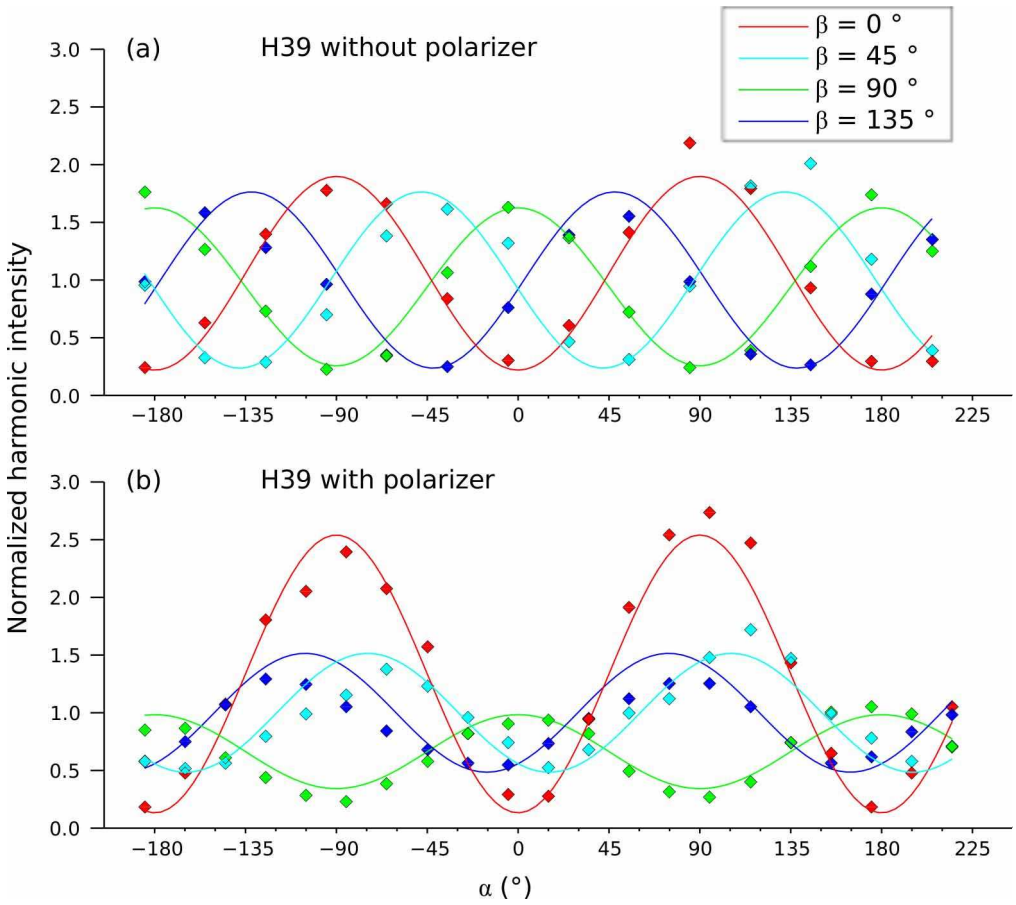

Fig. 3. Harmonic intensity as a function of α and β for the 39th harmonic at 20.9 nm. This harmonic is the closest to the wavelength for which the polarizer has been optimized (20.7 nm). The diamonds represent the measured data whereas the plain lines represent the best fit using Eq. (14). The intensity has been normalized by dividing the top curves (a) by I'_f in and the bottom curves (b) by I_f to allow a direct comparison between (a) and (b). The top graph (a) shows data recorded with the spectrometer only. It has a little effect on the polarization of the harmonic: the sinusoids have almost the same amplitude and their phase-shift is given by β. The bottom graph (b) shows data recorded with the spectrometer and the polarizer. The measured effects are mostly due to the polarizer. The curves obtained for $\beta = 45$ and 135 are almost in phase. This indicates that, as expected, the phase-shift induced by the polarizer is close to $\frac{\pi}{2}$ and that circularly polarized light can be obtained.

spectrometer itself has only a minor effect on the polarization of the 39th harmonic. Similar behaviors have been observed for all other harmonics as well.

When introducing the polarizer, a very different angular dependence is found (Fig. 3(b)). As expected, for each β angle a sinusoidal dependence on α is observed, but the phase shifts between the curves and their amplitudes have changed. The fact that the curves obtained for $\beta = 45$ and 135 are almost in phase indicates that the phase-shift induced by the polarizer is close to $\frac{\pi}{2}$. To extract more information, the data must be fitted with Eq. (14). The solid lines on Fig. 3 represent the best fits obtained. From these fits, the value of Ψ_a, Δ_a, Ψ'_a, Δ'_a, I_f, $I'_f$and Ψ_b

#139458 - $15.00 USD Received 9 Dec 2010; revised 30 Jan 2011; accepted 30 Jan 2011; published 22 Feb 2011

can be extracted. Using Eqs. (15), (16), and (17), the parameters r''_{pa}, r''_{sa}, Ψ''_a, Δ''_a are calculated. P_C^{Max} and T_C are then calculated using Eqs. (11) and (12). It has to be noted that the curves of Figs. 3(a) and 3(b) have been normalized, i. e. divided by I'_f and I_f respectively. Equation (14) shows that this normalized intensity can vary only between 0 and 4.

Table 1 summarizes the results obtained for each harmonic. First, some general trends can be observed. The reflectivities r''_{pa} and r''_{sa}, increase with harmonic order while the phase-shift decreases. This behavior is expected theoretically for molybdenum mirrors at glancing angles smaller than 30 and at wavelengths between 18 and 27 nm. As a result, the degree of circular polarization, P_C^{Max}, decreases with harmonic order. The circular transmission, T_C, follows an opposite trend up to the 39$^{\text{th}}$ harmonic. For higher order harmonics the *s* and *p* reflectivities are superior but the Ψ''_a and Δ''_a angles are smaller resulting in a reduced circular transmission compare to the 39$^{\text{th}}$ harmonic.

The 39$^{\text{th}}$ harmonic, at 20.9 nm, is the closest to the cobalt resonance at 20.7 nm. For this harmonic, the degree of circular polarization is 85 % and the circular transmission is 4.4 %. The theoretical values are 100 % and 7.9 % respectively. Imperfections of the mirrors (e. g. roughness, oxidation,) and small errors on the incidence angle of the polarizer could be responsible for these discrepancies. Indeed, a reduction of the reflectivity per mirror of 15 % would lead to a drop in transmission of the four mirror system of 50 %.

Nevertheless, this is a very good achievement. For example, with these characteristics it will be possible to measure the MCD effect at the cobalt *M*-edge. Indeed, using previous measurements for the generation of harmonics in two-color fields ($>$ 0.65 nJ at 20.9 nm, [2]), our polarizer could yield up to 30 pJ per impulsion or 30 nJ per second for the 39$^{\text{th}}$ harmonic at 20.9 nm with a very high degree of circular polarization. With such a power it would be very easy to measure the transmission of a 40 nm thick cobalt layer at the cobalt *M*-edge (transmission $>$ 1 %) very accurately. Doing so for both light helicity would give a measure of the MCD effect.

The results obtained for harmonics other than the 39$^{\text{th}}$ are also very impressive. For the 31$^{\text{st}}$ and 33$^{\text{rd}}$ harmonics the degree of circular polarization even reaches 100 %. To our knowledge, it is the first report of circularly polarized high order harmonics in the EUV range. The transmission of the polarizer for these 2 harmonics is superior to 2.5 %. The degree of circular polarization for the 35$^{\text{th}}$ harmonic is still very high at 97 % and the transmission is close to 4 %. This is particularly interesting for magnetic studies since the 35$^{\text{th}}$ harmonic is situated at the absorption *M*-edge of iron. In this regard, it has to be noted that the degree of circular polarization of the 41$^{\text{st}}$, 43$^{\text{rd}}$ and 45$^{\text{th}}$ harmonics and their circular transmission are still high. Then, it will be possible to probe the MCD effect at the absorption *M*-edge of nickel around 18.5 nm.

5. Conclusion

In this article, we showed that circularly polarized light in the EUV region can be generated efficiently at HHG source using a four mirror circular polarizer. A degree of circular polarization equal or close to 100 % was obtained for harmonics in the wavelength range on 18.1 to 26.3 nm with an efficiency between 2.6 and 4.4 %. With such a performance of these light sources, the MCD effect at the absorption M-edge of Fe, Co and Ni (at 23.8, 20.7 and 18.5 nm respectively) can be probed and used to study nanoscale ultrafast magnetic dynamics. For the time being, this type of studies can be conducted at only a few places worldwide. We hope that the use of circular EUV light from HHG sources will open this field of study to a wider community.

Other applications will benefit from a circularly polarized coherent EUV light source. First, it can be used in FEL or in laser plasma amplifier as a seed to obtain circularly polarized amplified light. There are other approaches to obtain circularly polarized light with a seeded FEL but for

#139458 - $15.00 USD Received 9 Dec 2010; revised 30 Jan 2011; accepted 30 Jan 2011; published 22 Feb 2011

laser plasma amplifier using a circularly polarized seed is the only solution. Another application which could benefit greatly from a circularly polarized HHG source is the nanoscale dynamics of biological systems. Indeed, these systems often show structures that can be imaged only by circularly polarized light such as chiral domains. It will be possible to observe the dynamic of such structures at the nanoscale level with circularly polarized harmonics. Element specific imaging could even be performed.

Finally, it should be emphasized that our setup can be improved at least on two points. First in this report, the polarizer was optimized for a precise wavelength. The performance of the polarizer for other wavelengths are then suboptimal. Second, our attention was focused on the maximization of the degree of circular polarization. A less restrictive criterion, and often more useful for experiment, is the maximization of the number of circularly polarized photons yielded by the polarizer. This criterion implies smaller glancing angles and thus higher reflectivities. Theoretically, circular transmission close to 20 % could be obtained. We are currently building a more versatile polarizer to address these two important points.

Acknowledgements

Financial support for this work was partially provided by the RTRA project IMMAGE and by the ANR project FEMTO-X-MAG.

#139458 - $15.00 USD Received 9 Dec 2010; revised 30 Jan 2011; accepted 30 Jan 2011; published 22 Feb 2011